

Fermi National Accelerator Laboratory

FERMILAB-Pub-97/021

Summary Report of the Intensity Limitations Working Group

Weiren Chou

*Fermi National Accelerator Laboratory
P.O. Box 500, Batavia, Illinois 60510*

February 1997

Submitted to *Particle Accelerators*

Presented at the *3rd International LHC Workshop*, Montreux, Switzerland, October 13-18, 1996

Operated by Universities Research Association Inc. under Contract No. DE-AC02-76CH03000 with the United States Department of Energy

Disclaimer

This report was prepared as an account of work sponsored by an agency of the United States Government. Neither the United States Government nor any agency thereof, nor any of their employees, makes any warranty, expressed or implied, or assumes any legal liability or responsibility for the accuracy, completeness, or usefulness of any information, apparatus, product, or process disclosed, or represents that its use would not infringe privately owned rights. Reference herein to any specific commercial product, process, or service by trade name, trademark, manufacturer, or otherwise, does not necessarily constitute or imply its endorsement, recommendation, or favoring by the United States Government or any agency thereof. The views and opinions of authors expressed herein do not necessarily state or reflect those of the United States Government or any agency thereof.

Distribution

Approved for public release; further dissemination unlimited.

SUMMARY REPORT OF THE INTENSITY LIMITATIONS WORKING GROUP

WEIREN CHOU

Fermilab, P. O. Box 500, Batavia, IL 60510, USA

(Received 29 January 1997; in final form ? 1997)

This paper summarizes the findings of the Intensity Limitations Working Group at the LHC96 Workshop. Discussions are focused on the three synchrotrons in the injector chain of the LHC, namely, the PSB, the PS and the SPS. Potential bottlenecks for reaching the nominal as well as the ultimate LHC beam intensity are identified and possible solutions are suggested. In addition, a comparison of proton synchrotron performance and a survey of machine impedance and simulation codes for instability studies are presented.

KEY WORDS: hadron collider, proton synchrotron, intensity, emittance

1 INTRODUCTION

The LHC is a high energy, high luminosity proton-proton collider. At 14 TeV center-of-mass energy, its nominal luminosity is $1 \times 10^{34} \text{ cm}^{-2}\text{s}^{-1}$. The ultimate luminosity (at the beam-beam limit) is 2.5 times higher than the nominal value. Such high luminosity requires beams of high brightness, *i.e.*, of high intensity and small emittance. When reduction due to the crossing angle and filling factor are ignored, the luminosity can be expressed as follows:

$$\mathcal{L} = \left(\frac{\gamma c}{4\pi} \right) \cdot \frac{1}{\beta^* S_b} \cdot \frac{N^2}{\epsilon} \quad (1)$$

in which γ is the relativistic factor, c the velocity of light, β^* the lattice β -function at the collision point, S_b the bunch spacing, N the number of protons per bunch, and ϵ the normalized transverse emittance. The luminosity is proportional to N^2 until it reaches the beam-beam limit (*i.e.*, until the brightness N/ϵ reaches a constant value). Then \mathcal{L} would be proportional to N . At nominal luminosity, the required beam intensity is 1.05×10^{11} protons per bunch, while at the ultimate luminosity, 1.6×10^{11} per bunch. The charge to this working group is to study the feasibility of the LHC injector chain for delivering beams at such intensities.

There are a number of sources that could limit the intensity of the beam. These include the space charge, transition crossing, microwave instability, mode-coupling instability, coupled bunch instability, resistive wall, static and transient beam loading, rf power, physical and dynamic apertures, rf gymnastics (*e.g.*, debunching,

rebunching and coalescing), particle loss and radiation shielding, intrabeam scattering and residual gas, *etc.* For each machine, some effects play more important role than the others. For example, the beam intensity in the Main Ring of Fermilab is severely limited by its aperture. This is one of the main reasons for replacing it by the Main Injector, which is under construction.

The LHC injector chain consists of four machines: the linac, the PS Booster (PSB), the PS and the SPS. During two days of work in this working group, we did not launch an all-out investigation on the phenomena listed above. Instead, we contented ourselves with the issues that appear to be most restrictive to the performance of the three synchrotrons. Namely, the new rf system in the PSB, longitudinal emittance budget and particle losses at extraction in the PS, and microwave and longitudinal coupled bunch instabilities in the SPS.

2 PERFORMANCE COMPARISON OF PROTON SYNCHROTRONS

In order to get an idea about how much room there could be in improving machine performance, it is listed in Table 1 comparisons of existing and planned proton synchrotrons. This is a updated version of a table presented to a previous workshop¹.

TABLE 1: Performance comparison of proton synchrotrons.

Machine	E_{\max} GeV	N_{tot} 10^{12}	N 10^{12}	A eVs	ϵ^h/ϵ^v μ	N/ϵ $10^{10}/\mu$	$N/(A\epsilon^h\epsilon^v)$ $10^{10}/\text{eVs}\cdot\mu^2$
<i>Existing:</i>							
BNL AGS	24	63	8	4	10/10	80	2
CERN PS	14	25	1.25	0.7	12.5/10	11	1.4
CERN SPS	450	46	0.012	0.5	10/7	0.14	0.03
KEK PS	12	3.6	0.4	2	5/15	4	0.27
FNAL Booster	8	4	0.05	0.1	3/3	1.7	5.6
FNAL MR	150	20	0.03	0.2	2/2	1.5	3.8
DESY III	7.5	1.2	0.11	0.09	5/3	2.8	8.1
PETRA II	40	5	0.08	0.12	8.7/6.2	1.1	1.2
<i>Planned:</i>							
AGS for RHIC	25	0.4	0.4	0.3	1.5/1.5	27	59
PS for LHC	26	14	0.9	1.0	2.8/2.8	32	11
SPS for LHC	450	24	0.1	0.5	3.5/3.5	2.9	1.6
FNAL MI	150	60	0.12	0.1	2/2	6	30
KEK JHP	50	200	12.5	5	55/55	23	0.08
$\mu\mu$ Proton Dr	30	100	25	4	50/50	50	0.25

In the table, E_{\max} is the maximum energy, N_{tot} the total number of protons. N the number of protons per bunch, A the 95% longitudinal emittance, ϵ^h and

ϵ^v the normalized transverse *r.m.s.* emittance in horizontal and vertical plane, respectively, N/ϵ the transverse density or beam brightness, and $N/(A\epsilon^h\epsilon^v)$ the 6-D phase space beam density. Usually high brightness directly translates to high luminosity. But sometimes the 6-D density can be a better indicator in performance comparison, especially if the bunch length is significantly different in different machines.

The goal of machine upgrade (e.g., AGS, PS, SPS and MI) is always to increase the 6-D density, but not necessarily the brightness. The ratio of the 6-D density before and after the upgrade represents the relative amount of work that would be required. From Table 1, it is seen that this ratio ranges from 8 (CERN PS) to 53 (CERN SPS).

3 THE PS BOOSTER (PSB)

3.1 The new rf system

For the LHC operation, the PSB will replace its present $h = 5$ cavities by $h = 1$, and there will be two injections from each of the four PSB rings into the PS, which will operate at $h = 8$. The present second harmonic cavities ($h = 10$) in the PSB, which are used for improving the bunching factor, will also be replaced by $h = 2$ cavities. The first pair of $h = 1$ and 2 cavities have been installed for demonstration and the experiment was successful. There should be no problem with this new rf system to reach the nominal LHC beam intensity. However, further studies are needed to see if this system is feasible at the ultimate LHC beam intensity. In particular, it is an unknown territory whether or not this system could be used for high intensity non-LHC beams, which are planned for fixed target and other PSB physics programs and need an intensity as five times high as that of the ultimate LHC beams.

One problem that has not yet been fully understood is the bunching factor gain when a second harmonic cavity is employed. F. Pedersen presented the theoretical prediction of the bunching factor (B_F) improvement with respect to the voltage ratio of the first and second harmonic cavities ($a_2 = V_2/V_1$), as shown in Figure 1. It is seen that, when a_2 is below 0.67, B_F increases approximately linearly with a_2 . Further increase of a_2 only leads to small increase in B_F . Therefore, $a_2 = 0.67$ seems to be an appropriate choice. At this ratio, the gain in B_F is expected to be about 37%. However, for some reason that is not clear, the real gain is smaller. The PSB rf group will continue its study on this problem.

3.2 H^- injection

The scheme of H^- injection has been adopted at Fermilab, BNL and DESY. But it is not used at CERN at this moment. S. Holmes pointed out that its main purpose is to increase the beam brightness N/ϵ in the first circular accelerator to the space charge limit with modest linac current. The space charge limit can be illustrated

in Figure 2, using Fermilab Booster as an example. At low intensity, the emittance remains a constant when the intensity increases. When the space charge limit is reached, the emittance increases with the intensity while keeping their ratio N/ϵ a constant. This explains the kinks in the figure. It also means the space charge tune shift, which is proportional to this ratio, becomes a constant after the limit is reached. Figure 2 shows two different space charge limits corresponding to two linac injection energies (200 and 400 MeV, respectively). The limit is proportional to $\beta\gamma^2$. In the case of PSB, it was concluded that, for the time being, H^- injection would not help to increase the brightness, because the space charge limit is already reached. However, with a possible linac upgrade in the future (for example, a 2 GeV linac discussed during the workshop), H^- injection could be a favorable option.

4 THE PS

There is no foreseen problems in transverse planes in the PS for the LHC beam. There are, however, two issues that need to be addressed in the longitudinal plane.

4.1 The Longitudinal emittance

The budget of the longitudinal emittance ϵ_L in the PS is tight. In the present design, it is 16 eV-s at injection (*i.e.*, 2 eV-s per bunch for 8 bunches), 26 eV-s during debunching, and 30 eV-s at extraction (*i.e.*, 0.35 eV-s per bunch for 84 bunches). Hence, there is only a factor of two allowed in emittance dilution. There are three constraints in the phase space, which are illustrated in Figure 3 by three boundaries. (i) The momentum acceptance in the PS extraction channel, which is about 6×10^{-3} ; (ii) The SPS microwave instability threshold at injection; and (iii) The SPS beam loading limit (which limits the bunch length due to phase modulations caused by the gaps in the SPS bunch train).

In addition to (i), the maximum allowable emittance is also limited by the available rf voltage V for providing needed bucket area A , which is:

$$A = \frac{1}{f_0} \sqrt{\frac{32eE}{\pi^3 h^3}} \sqrt{\frac{V}{\eta}} \quad (2)$$

where f_0 is the revolution frequency, E the beam energy, h the harmonic number and η the slip factor. When everything else is fixed, the bucket area is proportional to $\sqrt{V/\eta}$. In other words, a small slip factor can compensate for the shortage of rf voltage. Therefore, there was a discussion about a new PS lattice that could give a smaller η and, in turn, allow for a larger ϵ_L .

4.2 The extraction kicker rise-time

The finite rise-time of the extraction kicker in the PS brings about two problems: (i) particle losses (loss of a few bunches during the rise-time); (ii) poor beam quality

of the bunches that are nearby the lost ones. The former leads to radiation concerns in the PS, while the latter could give rise to problems to the physics experiments in the LHC.

A number of schemes of how to generate a gap in the PS bunch train were discussed. The following are two examples:

4.2.1 Three batch injection This is shown in Figure 4 by R. Garoby. It involves four stages.

(a) *Beam transfer from the PSB to the PS:* The PSB operates at $h = 1$, the PS at $h = 11$. The first batch inject 4 bunches into the PS, one from each PSB ring. So does the second one. The third batch inject only 2 bunches into the PS. Thus one bucket is left empty.

(b) *Splitting:* The PS changes $h = 11$ to $h = 22$, and each bunch is split to two. Thus there are 20 bunches and 2 empty buckets.

(c) *Squeezing:* The PS changes $h = 22$ to $h = 21$, resulting in 20 bunches and one empty bucket.

(d) *Splitting again:* The PS changes $h = 21$ to $h = 42$ and then to $h = 84$. The final outcome is 80 bunches and a gap of 4 buckets.

4.2.2 Longitudinal chopping There is a RFQ in the linac. It has a useful feature, namely, highly selective in the injection energy. Both simulations and measurements show that a few keV energy error could alter the transmission coefficient from above 90% down to virtually zero^{2,3}. Therefore, by applying a pulsed high permeability ferrite ring in front of the RFQ, one may vary the beam energy by a few keV and thus generate a gap in the linac particle sequence. This pulsed ring serves as a longitudinal chopper. Compared with the commonly used transverse choppers, its main advantage is the short physical length (a small fraction of that of the transverse ones). This is especially important in preserving the beam emittance in the low energy beam transfer line, where the space charge has dominant effects. Although this scheme is not applicable in the present injector chain $\text{linac} \rightarrow \text{PSB} \rightarrow \text{PS}$, it could be useful for generating gaps in the proposed 2 GeV $\text{linac} \rightarrow \text{PS}$ injection.

In addition to these two methods, other possible tactics include a wideband anti-damper (slowly kicking several selected bunches out before extraction), a fast kicker (with short rise-time) and barrier buckets.

5 THE SPS

The main problems of the SPS appear to be longitudinal instabilities, both single bunch and coupled bunch.

5.1 Microwave instability

5.1.1 At $\epsilon_L = 0.6$ eV-s Figure 5 is the SPS microwave instability threshold calculated by using the Keil-Schnell criterion. The broadband impedance model is assumed to be: $Z/n = 20 \Omega$, $f_r = 1.3$ GHz, $Q = 0.99$. The longitudinal emittance is 0.6 eV-s. It is seen that after 4 seconds in the cycle, beam would become unstable at the nominal LHC intensity of 1×10^{11} . However, it is known from J. Gareyte's experiment that, at 315 GeV (roughly around 6 seconds in the figure), a beam at 1.5×10^{11} is perfectly stable. This is about a factor of 2.5 higher than the threshold predicted by the curve. There are two ways to possibly explain this discrepancy.

(i) Keil-Schnell criterion: The criterion (and its Boussard modification) has uncertainties in its predicted value of the instability threshold. It is probably only good within a factor of two or so.

(ii) Impedance model: The broadband resonator model also has its limit in applications. E. Shaposhnikova recently conducted a series of impedance measurements using beams in the SPS and is in the process to establish a better impedance model for further analysis. She successfully identified the sources of a number of resonant peaks in the impedance spectrum and pointed out that the main contributors are the rf cavities, kickers and vacuum ports.

5.1.2 At $\epsilon_L = 1$ eV-s Figure 6 is the microwave instability threshold corresponding to a longitudinal emittance of 1 eV-s. It is seen that, at the nominal LHC beam intensity, there would be no instability. Obviously a large emittance could make the beam more stable. However, this is not the preferred solution. There are two reasons:

(i) Large ϵ_L leads to small dynamic aperture at injection of the LHC. This is shown by J. Gareyte in Figure 7. He indicated that the emittance from the SPS should be in the range between 0.5 and 1 eV-s.

(ii) Even at 1 eV-s, the SPS would have to perform bunch compression at the end of the cycle in order to shorten the bunch due to beam loading considerations. Such a process would require a new 400 MHz rf system.

Therefore, the preferred solution is to maintain the beam emittance at about 0.5 eV-s (thus no need of bunch compression) while keeping the microwave instability under control. There were two proposals:

(i) T. Linnecar proposed to program the transition energy γ_t during the cycle, because the threshold is proportional to the slip factor η , which is proportional to γ_t^{-2} .

(ii) E. Shaposhnikova proposed to rebuild the vacuum ports in order to lower the impedance.

5.2 Longitudinal coupled bunch instability

The growth time of the longitudinal coupled bunch instability is estimated at about 200 ms for each 1 M Ω shunt impedance of the higher order modes (HOM) of rf cavities. There are several types of existing rf cavities in the SPS: travelling

wave (TW) 200 MHz, superconducting (SC) 400 MHz, TW 800 MHz, *etc.* It has been planned to build longitudinal feedback systems to damp the mode 1 and 2 instabilities. Furthermore, if the new 400 MHz system would be installed for the purpose of bunch compression, it will use SC cavities and the HOM will be better damped so that no new feedback systems would be required.

During the LHC operation, the SPS will only be partially filled (3/11). But the known instability theories are based on the assumption that all the bunches are equally spaced. There was a discussion on how to estimate the growth time of a partially filled ring. It was found that innovative work is needed on this important subject.

6 OTHER DISCUSSIONS

6.1 2 GeV linac

R. Garoby proposed a new 2 GeV linac in the LHC injector chain to replace the existing linac and PSB. This proposal has a number of appealing features:

- (i) Reuse of the LEP SC cavities, which will be decommissioned after the LEP physics programs are completed.
- (ii) No need of debunching and rebunching in the PS.
- (iii) Possible adoption of H^- injection.
- (iv) Possible employment of longitudinal chopping.
- (v) High beam brightness that will lead to high luminosity (until the beam-beam limit is reached).

6.2 Computer codes for impedance and instability studies

Table 2 is a list of computer codes that have been used in the accelerator community for impedance and instability studies. Several codes for longitudinal dynamics and space charge effect studies are also included.

TABLE 2: Computer codes. ([]: code no longer supported)

Impedance		Instability		Longi. dynam.	Space charge
2-D	3-D	Analytical	Tracking		
TBCI	Mafia	BBI	Simtrac	ESME	Simpson
ABCI	Argus	ZAP	Trisim	Long1D	Accsim
Urmel	HFSS	Moses			
BPERM	Opera	Vlasov			
Superfish	Eminince				
Seafish	[SOS]				
Slans					
[Xwake]					

6.3 Machine impedance

Table 3 is a list of the measured machine impedance and instability threshold of existing proton synchrotrons. As a comparison, the design values of the Fermilab Main Injector are also included. As a matter of fact, most accelerators designed and built since the 1980s (*e.g.*, MI, AGS Booster, RHIC and the lepton machines LEP, APS, ESRF, *etc.*) have a Z/n about one order of magnitude lower than those built in early years. This is because nowadays more attention is directed to the low impedance design than before, such as a uniform cross section of beam tubes, rf-shielded bellows, valves, flange gaps and pump ports, tapered transitions, damped HOM, metal-coated ceramic pipes, *etc.*

TABLE 3: Machine impedance and instability threshold.

Machine	Longi. imped. $Z/n, \Omega$	μ -wave insta. Ω	Trans. imped. $M\Omega/m$
PS	17 (@14 GeV)	40 (@26 GeV)	1.4
SPS	20 10 (@low freq.)	10-12	
AGS	20		
DESY III	10 (@7.5 GeV)	14	2.2
PETRA II	2	10-20	
MI	1.6	8 (@150 GeV) 1 (@debunching)	

6.4 Space charge and decoherence time

There was an interesting discussion about if space charge effects could lead to decoherence. A good estimate of the decoherence time is important in the design of injection dampers. It was observed in the SPS that decoherence is fast (about 20 turns) and has dependence on beam intensity and energy. Moreover, the calculated space charge tune shift seems to support the measured value of decoherence time. Therefore, it was suggested that decoherence in the SPS was due to space charges. However, R. Baartman gave an elegant argument that any direct space charge effect could not lead beam to decohere. Other sources, such as chromaticity and octupoles, are unlikely the causes either, because the observed decoherence has intensity dependence and the SPS is very linear. Thus, it remains to be a puzzle what is the origin of this phenomenon.

7 CONCLUSIONS

The potential bottlenecks for reaching the LHC beam intensity in the injector chain have been investigated. A number of further studies are suggested for each of the

three injectors:

- PSB: Experiments with the $h = 1$ and $h = 2$ rf system.
- PS: (i) Longitudinal emittance budget and control; (ii) generation of a gap in the bunch train.
- SPS: (i) Better machine impedance models; (ii) rebuild of some critical vacuum parts for lower impedance; (iii) feasibility of γ_t programming during the cycle; (iv) instability analysis of a partially filled ring.

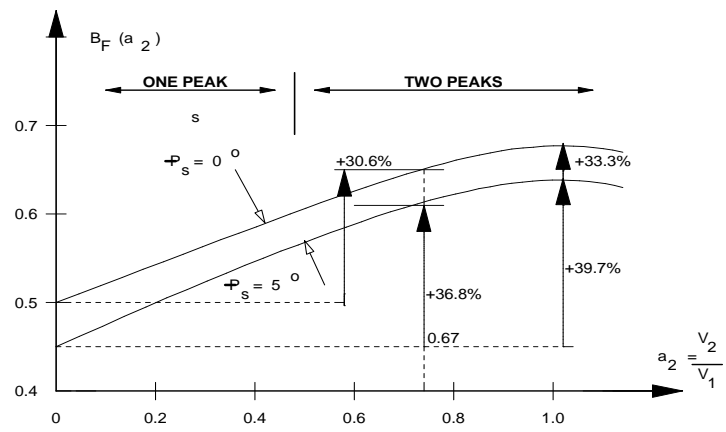
Generally speaking, it seems there is no real show stopper in these machines on their way marching towards the nominal as well as the ultimate LHC beam intensity.

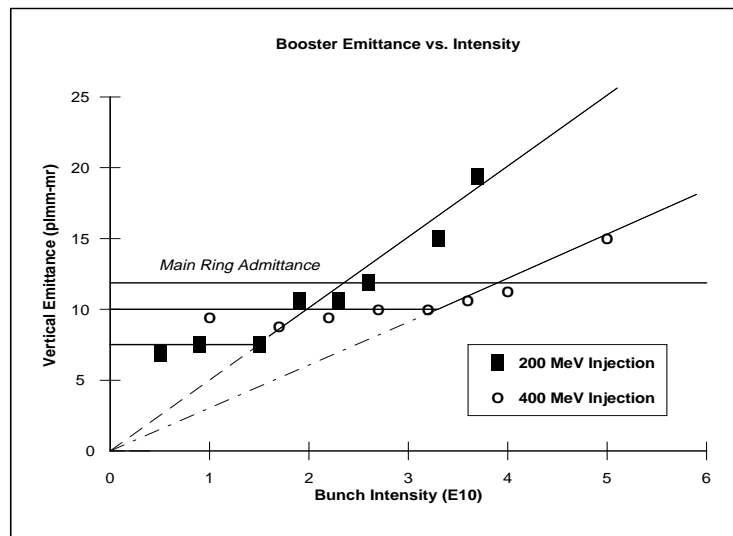
ACKNOWLEDGEMENTS

I am thankful to the members of this working group for their well-prepared presentations and stimulating discussions. Special gratitude is due to E. Keil and the Organizing Committee. In particular, I am deeply indebted to O. Brüning and J. Thomashausen. Without their invaluable help and cooperation, it would be impossible to make the working group a pleasant success.

REFERENCES

1. P. Martin and W. Chou, *Report of the Transition Crossing Mini-Workshop*, May 20-23, 1996 at Fermilab, Fermilab-TM-1979 (July 1996)
2. W. Chou, *Variable Bunch Spacing in Super Collider*, Proc. 1995 IEEE Particle Accelerator Conference, Dallas, May 1-5, 1995, p. 440
3. A. Ueno, KEK, private communication

FIGURE 1: Bunching factor *vs.* rf voltage ratio.

FIGURE 2: Fermilab Booster vertical emittance *vs.* bunch intensity.

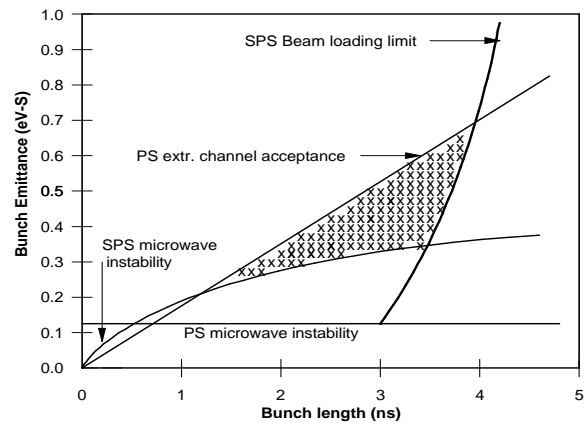


FIGURE 3: Constraints in the PS longitudinal phase space.

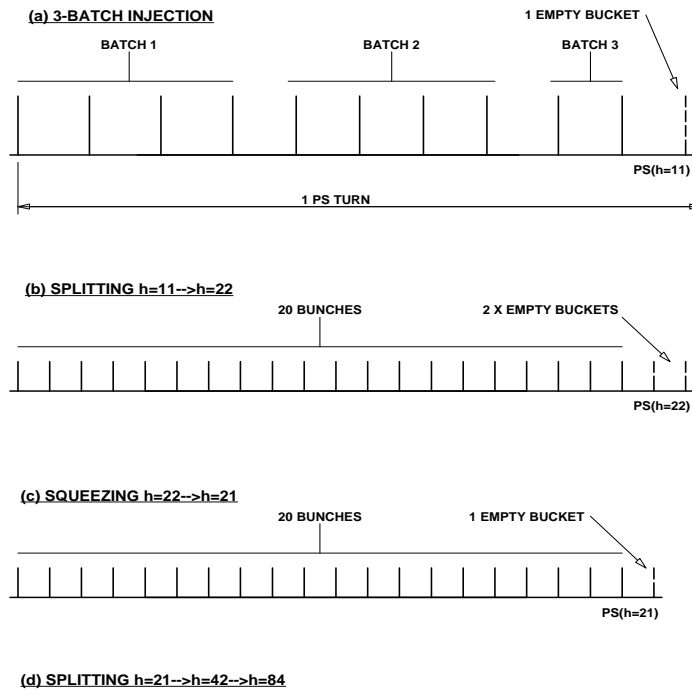


FIGURE 4: Three batch injection from the PSB to the PS.

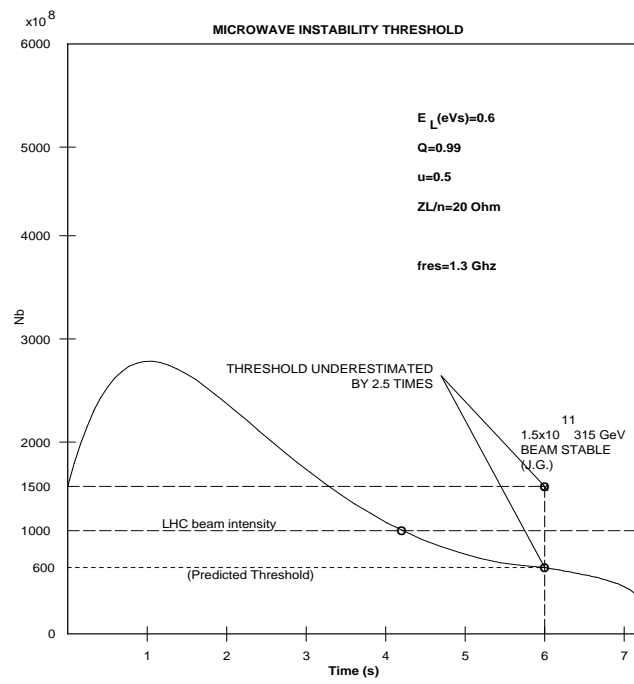
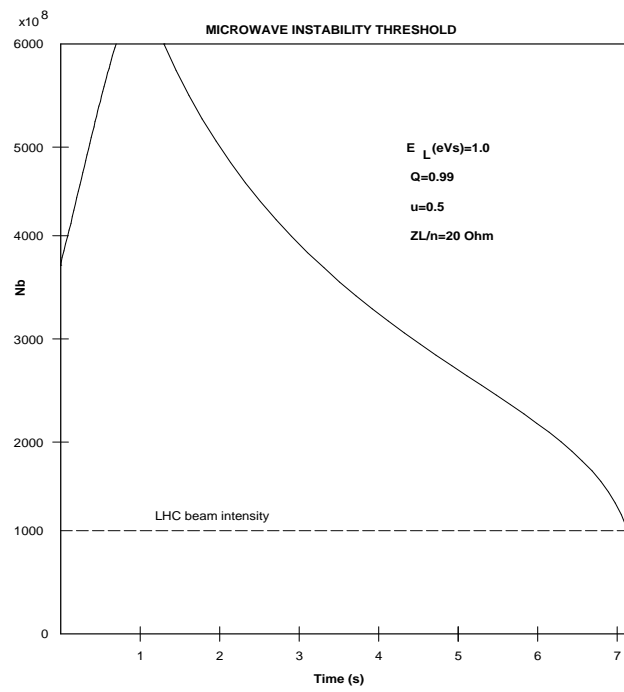
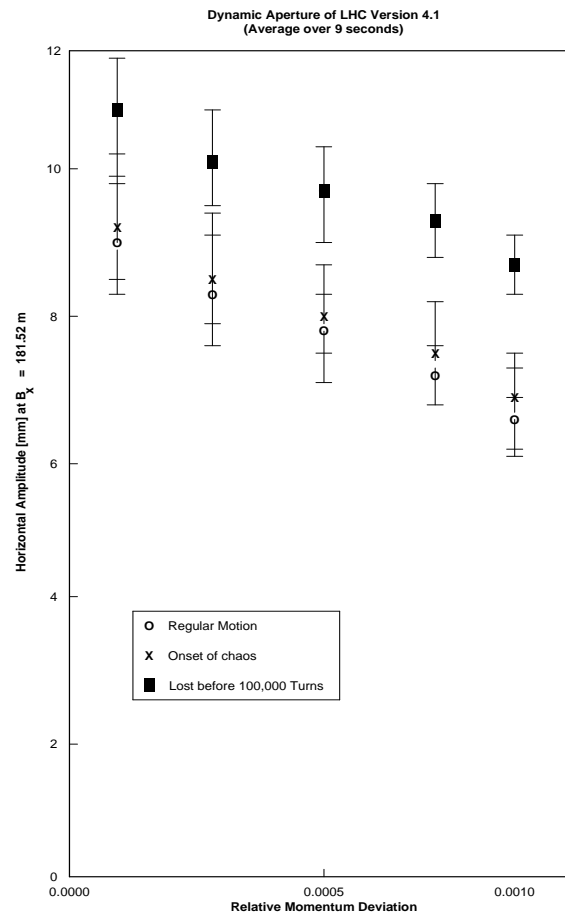


FIGURE 5: SPS microwave instability threshold at $\epsilon_L = 0.6 \text{ eV-s}$.

FIGURE 6: SPS microwave instability threshold at $\epsilon_L = 1 \text{ eV-s}$.

FIGURE 7: LHC dynamic aperture *vs.* relative momentum deviation.